

## Concentrations and sources of aerosol ions and trace elements during ANTICI-2003

R. Arimoto<sup>a,\*</sup>, T. Zeng<sup>b</sup>, D. Davis<sup>b</sup>, Y. Wang<sup>b</sup>, H. Khaing<sup>a</sup>, C. Nesbit<sup>a</sup>, G. Huey<sup>b</sup>

<sup>a</sup>Carlsbad Environmental Monitoring and Research Center, New Mexico State University, Carlsbad, NM 88220, USA

<sup>b</sup>School of Earth and Atmospheric Sciences, Georgia Institute of Technology, Atlanta, GA 30332, USA

Received 8 January 2007; received in revised form 18 April 2007; accepted 19 May 2007

### Abstract

As part of the Antarctic Tropospheric Chemistry Investigation (ANTCI), bulk aerosol-particle samples collected at the South Pole were analyzed for nitrate, sulfate, methanesulfonate (MSA), selected trace elements and radionuclides. The samples were collected in the same manner as in the Investigation of Sulfur Chemistry in the Antarctic Troposphere (ISCAT) campaigns of 1998 and 2000. The ANTICI mean sulfate ( $124 \text{ ng m}^{-3}$ ) and MSA ( $9.1 \text{ ng m}^{-3}$ ) concentrations were comparable to those during ISCAT, but high MSA and sodium and high MSA/sulfate in late November/early December indicated pervasive maritime influences during that time. Trajectory analyses indicate that the Weddell Sea and the Southern Ocean near Wilkes Land were probable sources for the ocean-derived sulfate. The transport of marine air occurs mainly in the buffer layer or free troposphere, and the rapid oxidation of biogenic sulfur to  $\text{SO}_2$  appears to be the basis for the observed low MSA/sulfate ratios. Elements typically associated with mineral dust (Al, Fe, K) and other elements with continental sources (Pb, Sb, Zn) had higher concentrations during ANTICI than ISCAT. The mean filterable nitrate ( $\text{f-NO}_3^-$ ) concentration ( $280 \text{ ng m}^{-3}$ ) also was conspicuously higher than during ISCAT (39 and  $150 \text{ ng m}^{-3}$ ). Several peaks in  $\text{f-NO}_3^-$  were synchronous with those for MSA and sulfate, but some samples had high  $\text{f-NO}_3^-$  but neither high MSA nor sulfate. While there is some evidence that nitrate or nitric acid is transported to SP from distant sources, local emissions of nitrogen oxides from the snow are a far more important source overall.

© 2007 Elsevier Ltd. All rights reserved.

**Keywords:** Sulfur; Aerosol ions; Elements; Radionuclides; South Pole atmosphere

### 1. Introduction

One the major objectives for the Antarctic Tropospheric Chemistry Investigation (ANTCI) has been to better understand the dynamical and chemical processes that control the concentrations

of  $\text{HO}_x$ ,  $\text{NO}_x$ , sulfur species and related substances over the Antarctic plateau (Eisele et al., this issue). In this context, the study reported here focuses on new aerosol findings at South Pole (SP) generated during the intensive sampling period of ANTICI-2003. The results relate specifically to nitrogen and sulfur compounds found in aerosol samples, but we also briefly consider trace elements and three naturally occurring radionuclides because they provide further insight on possible origins of the aerosol N and S.

\*Corresponding author. Tel.: +1 505 234 5503;  
fax: +1 505 887 3051.

E-mail address: [arimoto@cemrc.org](mailto:arimoto@cemrc.org) (R. Arimoto).

Results from Investigation of Sulfur Chemistry in the Antarctic Troposphere (ISCAT) and other studies have shown that SP during the summer is characterized by unexpectedly active photochemistry. Driven by high concentrations of nitrogen oxide, NO, the SP atmosphere is strongly oxidizing. Although emissions of NO<sub>x</sub> from the snow have been shown to be the major source for this reactive nitrogen at SP (Davis et al., 2001, 2004), the question remains: what are the primary sources of the nitrogen found on the plateau? For example, in an examination of atmospheric transport to the plateau during ISCAT-2000, Arimoto et al. (2004a) found that on at least one occasion a high-pressure ridge caused a significant influx of air from beyond the Antarctic convergence to SP, and this was accompanied by highest loadings of several ocean-derived substances observed during the study. Those substances included methanesulfonate (MSA) (an oxidation product of the biogenic compound dimethyl sulfide, DMS), Na, Cl, as well as non-sea-salt sulfate (nss-SO<sub>4</sub><sup>2-</sup>, i.e., the sulfate in excess of that from sea-salt and which is typically also a major oxidation product of DMS).

In this study, we use trajectory analyses to investigate the transport pathways associated with high concentrations of sulfate, filterable nitrate and various other aerosol species, including Na, MSA, several trace elements from geological sources (Al, Fe, etc.), and other elements with strong continental sources (Pb, Sb and Zn). In addition, the activities of three naturally occurring radionuclides also were determined <sup>7</sup>Be (53-day half-life), <sup>210</sup>Pb (2-year half-life) and <sup>210</sup>Po (138-day half-life). <sup>7</sup>Be is produced in the upper troposphere/lower stratosphere through reactions of cosmic rays with oxygen and nitrogen (Gerasopoulos et al., 2003), and therefore it is a useful indicator of the downward mixing of air from those layers of the atmosphere. <sup>210</sup>Pb, a radon daughter, can be used as tracer of continental air (Balkanski et al., 1993), and <sup>210</sup>Po is a possible indicator of volcanic emissions (Su and Huh, 2002). Earlier studies for ISCAT (Arimoto et al., 2004a) included a preliminary evaluation of the contribution of volcanic emissions to the SP sulfur budget using data for <sup>210</sup>Po. A second paper (Arimoto et al., 2004b) considered in some detail aerosol Pb, which the data suggest may have decreased in concentrations since the 1970s, and also results for Hg, which showed levels approaching those in the Arctic but whose cycling evidently is driven by different processes. Results from Hg studies

conducted for ANTCI are presented in Brooks et al. (this issue).

## 2. Experimental

### 2.1. Sampling

An overview of the ANTCI project, including a statement of objectives, a summary of the measurements and highlights of the findings, is presented by Eisele et al. (this issue). For the aerosol studies reported here, 30 high-volume, bulk samples were collected on single Whatman 41<sup>TM</sup> filters (Whatman Ltd., Maidstone, UK) over ~24 h intervals using the same procedures as those in the ISCAT studies (Arimoto et al., 2001, 2004a, b). The samples were collected from 22 November to 22 December 2003 from the roof of the Clean Air Facility (89.997°S, 102.0°W, elevation 2841 m). The arithmetic mean volume of air sampled was 1661 m<sup>3</sup> (standard deviation, SD = 103 m<sup>3</sup>). As in ISCAT, a second high-volume sampler was used to collect samples for the analyses of <sup>7</sup>Be, <sup>210</sup>Pb and <sup>210</sup>Po.

One difference between ANTCI and the two ISCAT studies is that for ANTCI the samples were transported by ship and kept frozen during transit while for ISCAT they were shipped by air express and unfrozen. There is, unfortunately, no way to determine whether the difference in sample shipment procedures affected the concentrations of any substances of interest, especially nitrate. However, with reference to possible losses of nitrate during transport, a study by Schaap et al. (2004) showed that no evaporation of ammonium nitrate occurred, even at 35 °C. Their studies also showed that Whatman 41<sup>TM</sup> filters quantitatively collect both aerosol nitrate and gas-phase nitric acid, and therefore, we refer to the nitrate measured in our samples as “filterable nitrate” or f-NO<sub>3</sub><sup>-</sup>.

### 2.2. Chemical analyses of major ions, trace elements and radionuclides

For the analyses of sulfate, nitrate and MSA, the Whatman 41<sup>TM</sup> filters were cut into quarters, extracted in three steps with de-ionized (18 MΩ) water, and analyzed by ion chromatography (Dionex 500; Dionex Corp., Sunnyvale, CA). Trace elements were determined in separate portions of the filters after digestion with ultrapure H<sub>2</sub>O, HNO<sub>3</sub>, HF and H<sub>2</sub>O<sub>2</sub> in a microwave digestion unit (Model MDS 2100; CEM Corporation,

Matthews, NC). The concentrations of up to 33 elements were determined with a Perkin-Elmer Elan 6000 inductively coupled plasma mass spectrometer, but we consider only a subset of those elements here. Details of the sample preparation and analytical methods have been reported in Arimoto et al. (2001, 2004a, b).

The activities of three radionuclides were determined using methods also described in Arimoto et al. (2004a). The activities of  $^{210}\text{Pb}$  and  $^7\text{Be}$  were quantified in folded filters with the use of a high-purity germanium spectrometer for  $^7\text{Be}$  (477.6 keV) and a dual scintillation-detector spectrometer for  $^{210}\text{Pb}$  (46.5 keV).  $^{210}\text{Po}$  was determined using an Oxford Oasis alpha-spectroscopy system (Oxford Instruments Inc., Oak Ridge, TN) following a series of purification steps and plating the  $^{210}\text{Po}$  onto a nickel planchet. The activities of the radionuclides were mathematically back-corrected to those at the time of collection.

### 2.3. Back-trajectory analyses

As noted earlier, one of the objectives of this study was to evaluate the influence of long-range transport on the aerosol populations at the SP. To achieve this objective, a back-trajectory model was used in conjunction with the ANTCI chemical data (Zeng, 2005). In the current application, back-trajectories were computed every hour from 21 November to 31 December 2003. Arrival heights at the SP were set at 17 m, which is the height at which the aerosol sampler was located. For interpretive purposes, we limited the trajectory results to 7 days, reflecting both our concern about the growing uncertainty in trajectories based on longer time integrations and problems that can arise due to aerosol depositional losses during transport.

Meteorological fields were assimilated using the polar version of the Fifth-Generation NCAR/Penn State Mesoscale Model (MM5; Bromwich et al., 2001) with input to the model coming from the European Centre for Medium-Range Weather Forecasts/Tropical Ocean and Global Atmosphere (ECMWF TOGA) analysis dataset. The model domain consisted of  $81 \times 81$  grids with a horizontal spatial resolution of 80 km. The 27 vertical layers in the model extended up to 10 mb in terrain-following  $\sigma$ -coordinates. Ten of these layers were placed in the lowest 1 km to better simulate the polar boundary layer. Two months of meteorological data were archived from a series of 6-day assimilations with

the first-day data removed. Model-simulated-winds had an accuracy of  $\sim 0.8 \text{ ms}^{-1}$  and  $\sim 18^\circ$  (SD) compared to the observations at the SP.

The kinematic back-trajectory calculation is based on the following differential equation:

$$\frac{d\vec{S}}{dt} = \vec{V},$$

where  $\vec{S}$  is the distance displacement,  $t$  is the time and  $\vec{V}$  is the velocity vector. Several sensitivity studies were conducted to test the performance of the trajectory model. First, 15-day backward/forward tests were performed to validate the integration algorithm. For these tests, the end points of back-trajectories were used as the origins for trajectories run in the forward mode. A perfect match between the backward and forward trajectories would indicate that the model accurately calculated the movements of the air masses. However, there were several cases in which the back- and forward-trajectories differed, mainly due to the non-linearity of the wind fields. That is, the wind at the beginning of each time step was used to represent the mean wind for that time step. Wind velocities used in the backward and forward calculations for the same time step were therefore taken from two wind fields with a 1-min time gap. In those cases, the horizontal displacements were small during the first week but became larger with time; this reflects the fact that the uncertainties grew as the integration times increased, and this is the main reason we limited the trajectories to 7 days. The backward/forward sensitivity test also led to improvements in the calculations which were achieved by modifying the time step and time integration scheme.

A second set of sensitivity tests was conducted to optimize the time step used to calculate the trajectories. Although the results from these tests cannot be considered definitive, they demonstrate how the choice of time step can affect the final results. In these tests, the time steps were varied (10, 5, 2, 1 and 0.5 min) while all other variables were held constant. The back-trajectories were generally similar for the first 11 days but then began to separate, with a displacement up to 350 km at the end of 15 days. Backward/forward tests were then used to find the most reproducible back-trajectory calculation. Based on the sensitivity results above, we chose 1 min as the initial value for each time step.

A novel constraint used to adjust the time step was that based on the application of the

Runge–Kutta fourth-order integration algorithm (Press et al., 1992). The latter has been shown to be better than the linear time integration typically used. Since four predicted displacements were used to calculate the final displacement for each time step, we shortened the time step until the four ending points arrived at the same grid box to improve the calculation accuracy. This technique was particularly effective during strong wind shear and improved the results in the backward/forward tests. Other constraints such as the Courant criterion (Courant et al., 1928) in three directions were also applied to further adjust the time step.

### 3. Results and discussion

#### 3.1. Temporal trends in concentrations

The concentrations of sulfate (arithmetic mean  $124 \text{ ng m}^{-3}$ ) and MSA ( $9.1 \text{ ng m}^{-3}$ ) during ANTCI were comparable to those during the two ISCAT campaigns, and the MSA/nss-SO<sub>4</sub><sup>2-</sup> ratios ( $R$ ) for all three campaigns were generally similar (Figs. 1 and 2). There were, however, several days during ANTCI (29 November to 3 December) when much higher than average MSA concentrations and high  $R$  values occurred (see later discussion). Aside from the November/December ANTCI event, most of the other samples had  $R$  values between 0.01 and 0.09, averaging 0.07 (Fig. 3), similar to the earlier ISCAT studies. If one removes several outliers from this plot (i.e., those points with MSA concentrations  $> 3$  SD from the mean calculated only for samples with nss-SO<sub>4</sub><sup>2-</sup> concentrations between 120 and  $170 \text{ ng m}^{-3}$ , the latter being the range of the corresponding values of the outliers), the slope is 0.070 and the resulting  $r^2$  value 0.70. Including those outliers, increases the slope only slightly to 0.078 but decreases the  $r^2$  value to 0.45. Treating the outliers independently, the resulting regression of MSA versus nss-SO<sub>4</sub><sup>2-</sup> gives a slope of 0.18, still only slightly steeper than in the ISCAT studies. More to the point, even the highest  $R$  value calculated for SP is much lower than the ratios reported for coastal Antarctica where  $R$  typically ranges from 0.36 to 0.58 (Savoie et al., 1993; Berresheim and Eisele, 1998).

The high MSA concentrations and high  $R$  values during the brief November/December 2003 event (Fig. 3) suggest that maritime influences were strongest at that time, and as discussed below air mass back-trajectories for these data points support

a marine influence. An earlier assessment of  $R$  values observed in Antarctica (Davis et al., 1998) highlighted the fact that this ratio is not only influenced by temperature but also by several other factors, the most critical of these being the physical conditions where the DMS oxidation takes place, that is, aerosol/cloud conditions versus cold, dry, free-tropospheric air. The latter region has relatively low aerosol loadings, and thus the oxidation of DMS is most likely to take place in the gas phase (via OH radicals) as compared to the boundary layer where much of the oxidation can occur on sea-salt particles (Davis et al., 1998). Other possible influences on  $R$  include the preferential removal of MSA relative to nss-SO<sub>4</sub><sup>2-</sup> during transport as well as the possibility that both MSA and nss-SO<sub>4</sub><sup>2-</sup> are transported onto the plateau from low latitudes, where  $R$  is known to be small over large expanses of the ocean (Savoie et al., 1989; Saltzman et al., 1983).

Recent studies of snow from Dronning Maud Land by Kärkäs et al. (2005) showed that both MSA and nss-SO<sub>4</sub><sup>2-</sup> concentrations decreased exponentially with distance from the coast, but MSA decreased more rapidly: 64%/100 km for MSA versus 48%/100 km for nss-SO<sub>4</sub><sup>2-</sup>. Preferential removal of MSA to the snow relative to nss-SO<sub>4</sub><sup>2-</sup> would cause  $R$  to decrease with distance inland, but other studies in Victoria Land (Gragnani et al., 1998) have shown the opposite trend; that is, a faster rate of decrease for nss-SO<sub>4</sub><sup>2-</sup> with distance from the coast. Inspection of the ISCAT and ANTCI data shows that the MSA concentrations were far more variable than those of SO<sub>4</sub><sup>2-</sup>, suggesting that most of the variation in  $R$  is due to major shifts in MSA not nss-SO<sub>4</sub><sup>2-</sup>. This was especially true during ANTCI, when the relative standard error (the standard error divided by the arithmetic mean) was 0.16 for MSA versus 0.05 for SO<sub>4</sub><sup>2-</sup>.

The higher variability in MSA relative to SO<sub>4</sub><sup>2-</sup> is consistent with prior observations showing that the lower values for  $R$  at SP compared with coastal sites were due to the larger concentration differences for MSA compared with SO<sub>4</sub><sup>2-</sup>. Whether this is due to preferential removal, chemical processing, or additional sources for SO<sub>4</sub><sup>2-</sup> remains to be determined, but the results clearly imply some differences in the behavior of the two compounds. In the scenario of Davis et al. (1998), more boundary-layer oxidation on particles leads to higher values for  $R$ .

The arithmetic mean f-NO<sub>3</sub><sup>-</sup> concentration during ANTCI ( $250 \text{ ng m}^{-3}$ ) was considerably higher than

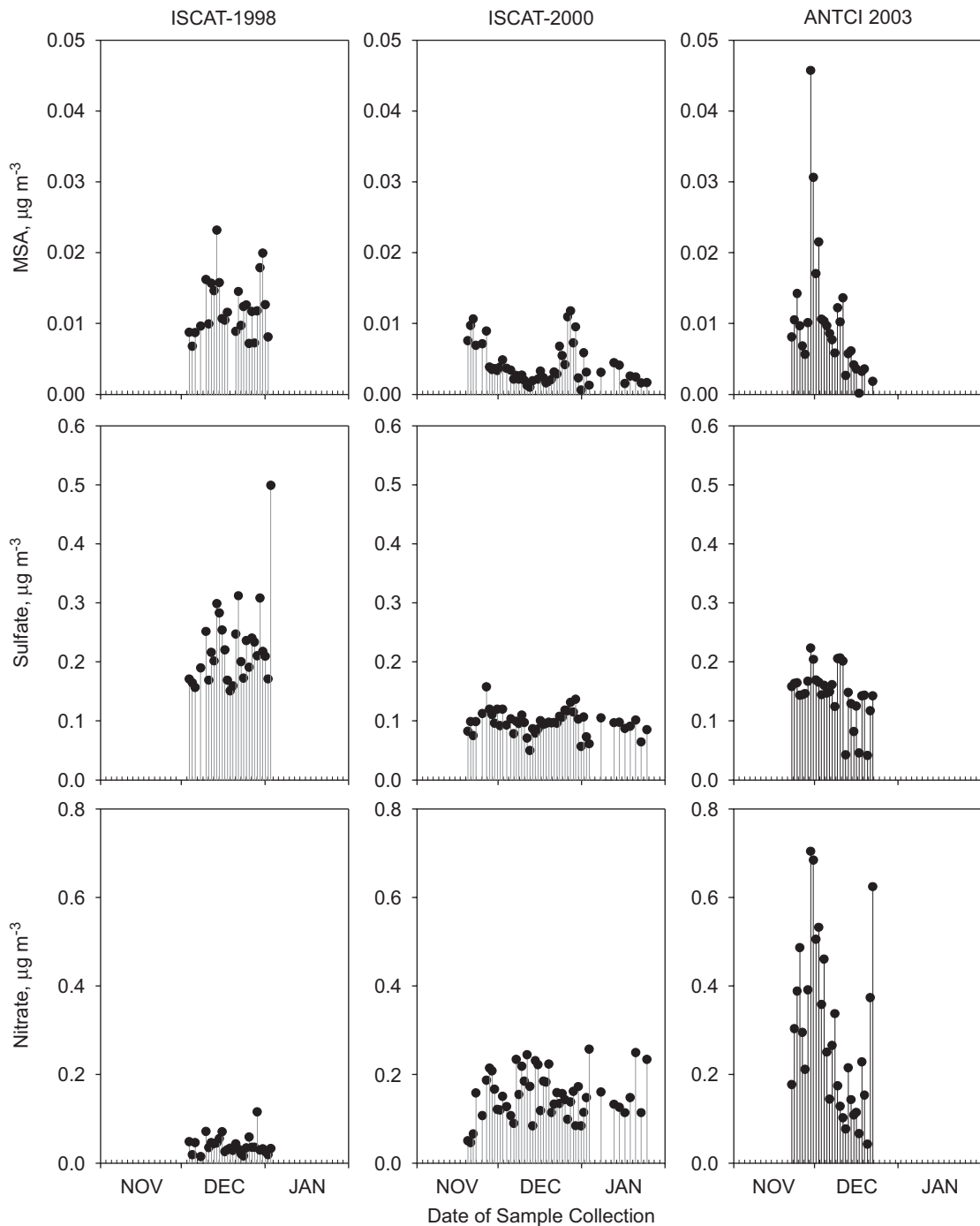


Fig. 1. Time-series plots for the concentrations of methanesulfonate (MSA), sulfate and nitrate in filter samples collected at the Clean Air Facility, South Pole.

that for either of the ISCAT data sets (39 and  $150 \text{ ng m}^{-3}$  for ISCAT 1998 and 2000, respectively, Fig. 1). Davis et al. (this issue) contrast the high plateau nitrogen levels with those near coastal areas, and further comparisons show that the

ANTCI  $\text{f-NO}_3^-$  was much higher than the nitrate collected on filters at Dome C (average  $10.6 \text{ ng m}^{-3}$  and maximum  $52.2 \text{ ng m}^{-3}$ , Udisti et al., 2004) or the total nitrate measured in Dronning Maud Land ( $20\text{--}50 \text{ ng m}^{-3}$  for samples collected in January and

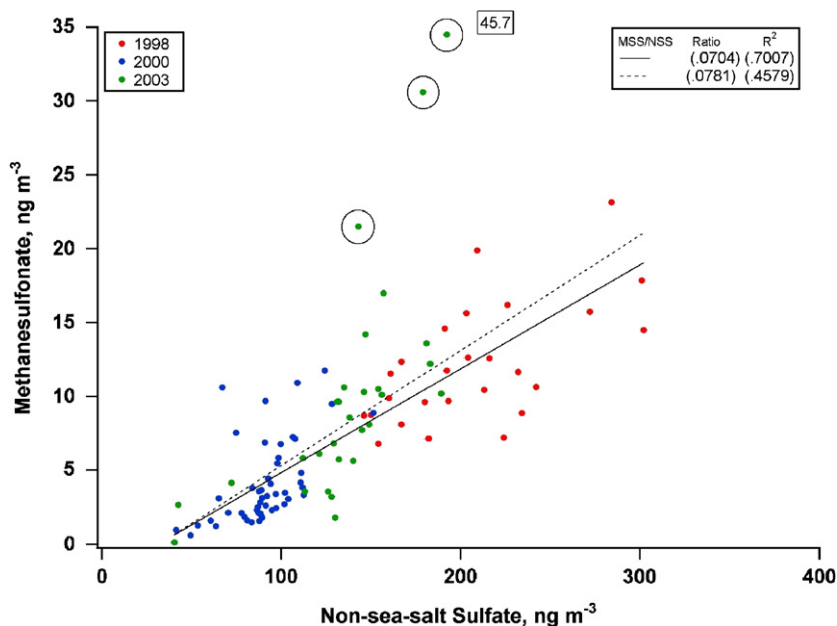


Fig. 2. Methanesulfonate versus non-sea-salt sulfate concentrations at the South Pole during ISCAT and ANTICI. Circled points show outliers.

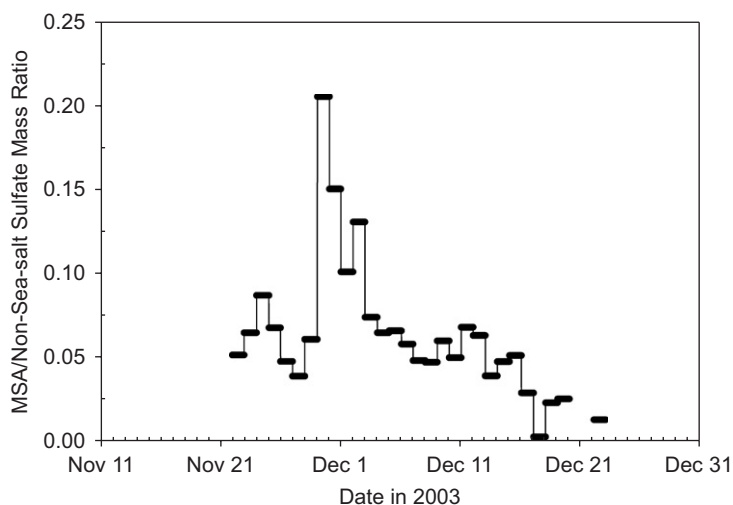


Fig. 3. Temporal variations in the mass ratio of methanesulfonate (MSA) to sulfate at the South Pole.

February 2000–2002, Piel et al., 2006). While some peaks in  $f\text{-NO}_3^-$  were synchronous with MSA and sulfate, the last two ANTICI samples collected (21–23 December 2003) had high  $f\text{-NO}_3^-$  but neither high MSA nor sulfate. As discussed later and in Sjostedt et al. (this issue) and Davis et al. (this issue), high concentrations of several gas-phase nitrogen species, including nitric acid, pernitric acid, NO and  $\text{NO}_y$ , also were found at this same time,

suggesting important influences of  $\text{NO}_x$  emitted from snow.

The concentrations of several elements typically associated with mineral aerosol, such as Al, Fe, K, etc., were roughly five times higher in the ANTICI samples compared with those collected during ISCAT-2000 (Table 1). Several other elements, including Pb, Sb, and Zn, that typically are dominated by continental sources also were higher

Table 1  
Summary statistics for trace element concentrations ( $\mu\text{g m}^{-3}$ ) in aerosol particles from the South Pole

Element	ANTCI			ISCAT-2000			Relative percent difference <sup>b</sup> (%)
	<i>n</i> <sup>a</sup>	Arithmetic mean	Standard error	<i>n</i>	Arithmetic mean	Standard error	
Aluminum	15	17.1	5.4	8	3.4	0.66	134
Antimony	8	0.10	0.03	7	0.009	0.002	168
Iron	12	54.4	7.9	3	7.7	1.7	151
Lead	29	0.18	0.04	15	0.03	0.01	141
Potassium	21	16.4	1.0	5	3.0	0.3	138
Sodium	27	75.5	4.6	11	9.9	1.5	154
Zinc	18	4.01	1.34	3	0.88	0.26	128

<sup>a</sup>*n*: number of samples.

<sup>b</sup>Relative percent difference is calculated as the difference in the arithmetic means (ANTCI–ISCAT-2000) divided by the average of the two means.

during ANTCI than in the previous studies. The trace-element indicators therefore suggest that there was more transport of continentally derived aerosol to SP during ANTCI than during ISCAT-2000.

### 3.2. Chemistry and transport: trajectory analyses

#### 3.2.1. Sources of $f\text{-NO}_3^-$

Local production now appears to play the dominant role in the nitrate chemistry at the SP, and the coupling between local nitrogen chemistry and  $f\text{-NO}_3^-$  during ANTCI is demonstrated by a scatter plot of the observed NO, which has a short atmospheric lifetime, versus  $f\text{-NO}_3^-$  (Fig. 4). The high correlation ( $r^2 = 0.76$ ) between NO and  $f\text{-NO}_3^-$  suggests that photochemistry makes a major contribution to  $f\text{-NO}_3^-$  (see also discussion by Davis et al., this issue). It also implies that  $\text{NO}_x$  emitted from the snow-pack is effectively converted into nitric acid, some of which is then converted to nitrate aerosol. As noted earlier, because our  $f\text{-NO}_3^-$  also includes trapped gas-phase  $\text{HNO}_3$ , it is reasonable to assume that most of the high values for this quantity reflect plateau-generated  $\text{HNO}_3$  and very likely also  $\text{HONO}_2$ . Both the gases have lifetimes of only a half-day to a day due to rapid removal via dry deposition.

Again, however, we are careful to note that uncertainties do exist in the  $f\text{-NO}_3^-$  measurements. In particular, under the extremely cold conditions at SP, nitric acid is believed to be “sticky” and to attach itself to the sample filters, becoming part of the nitrate determined by ion chromatography (Fig. 5). At this point, the exact fraction of the filterable nitrate that is  $\text{HNO}_3$  is unknown, and this

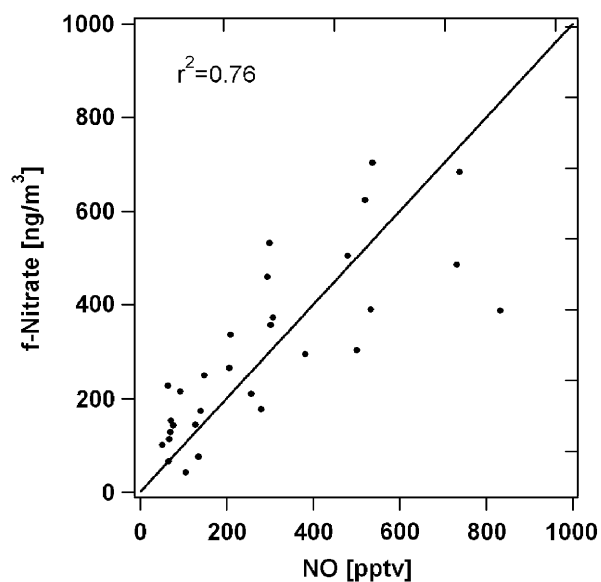


Fig. 4. Observed NO and filterable nitrate at the South Pole during ANTCI.

complicates the interpretation of our filter data. A conclusion from the Schaap et al. (2004) study cited above was that Whatman 41<sup>TM</sup> filters quantitatively collect nitric acid, but in two of the ANTCI samples (12–13 and 20–21 December),  $\text{HNO}_3$  apparently was higher than  $f\text{-NO}_3^-$ , suggesting that  $\text{HNO}_3$  is not always collected quantitatively. Interestingly, the  $f\text{-NO}_3^-$  concentrations in those samples were among the lowest of the sample set, and they also had low concentrations of the marine indicators, MSA and Na.

Prior studies (Maenhaut et al., 1979; Arimoto et al., 2001) have shown that the Cl/Na mass ratio in

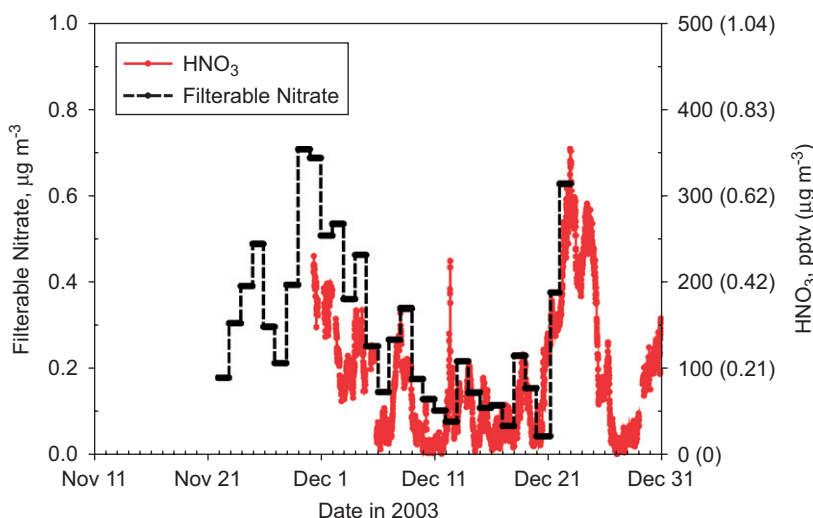


Fig. 5. Variations in nitric acid and filterable nitrate during ANTCL.

the SP aerosol samples is lower than in fresh sea-salt aerosol particles, with depletions of roughly 40–60%. Dechlorination can occur following sorption of  $\text{HNO}_3$ , acidification of the sea salt and loss of HCl (Brimblecombe and Clegg, 1988). These two observations suggest that the uptake of  $\text{HNO}_3$  and its contribution to  $\text{f-NO}_3^-$  may be related to the amount of sea salt collected on the filters, but as discussed below, it also may be a manifestation of large-scale differences in the composition of the air masses. Taking 50% as a representative value for Cl depletion, one can show that up to  $\sim 35\%$  of the  $\text{f-NO}_3^-$  measured could be associated with sea salt. This is arguably an upper limit because other substances may have contributed to the observed Cl depletion, but it does represent an appreciable fraction of the  $\text{f-NO}_3^-$ .

The long-range transport of anthropogenic nitrate and the influx of stratospheric nitrate (Wagenbach et al., 1998) are other possibly important sources of primary nitrogen that would appear as  $\text{f-NO}_3^-$  at SP, but these influences are difficult to evaluate quantitatively. Even so, with respect to the latter, the activities of  $^7\text{Be}$  (an indicator of upper tropospheric/lower stratospheric air) and concentrations of  $\text{f-NO}_3^-$  were not significantly correlated ( $r = -0.27$ ), suggesting that other sources were more important determinants of  $\text{f-NO}_3^-$ , and therefore, the stratospheric source is not considered further here.

The role of transport as a source of primary nitrogen is likely significant for some specific events; but it is perhaps more important to consider this

source in the larger/longer term context of the nitrogen budget for the whole of Antarctica. When the atmosphere over the Antarctic plateau is viewed as a system, both recycling from snow and the influx of primary nitrate from distant sources are potentially important determinants of the observed  $\text{f-NO}_3^-$ . As noted by Davis et al. (this issue), recycling evidently is sufficiently large that one is led to the conclusion that a very large fraction of the  $\text{NO}_x$ ,  $\text{HNO}_3$  and  $\text{HO}_2\text{NO}_2$  observed at a given time is due to recycled nitrogen or secondary  $\text{NO}_x$ . There are difficulties, however, in trying to sort out the contributions from local versus remote primary sources for  $\text{f-NO}_3^-$  because local  $\text{NO}_x$  (and hence  $\text{HNO}_3$ ) levels can fluctuate dramatically over short periods of time due to shifts in meteorology such as changes in planetary boundary layer (PBL) height.

In an effort to understand this complicated setting and to evaluate the importance of distant sources for reactive nitrogen, we employed back-trajectory analyses to see if evidence could be found for a contribution to  $\text{f-NO}_3^-$  from long-range transport. As discussed later, this effort was combined with an assessment of the trends in sulfur compounds that are known to primarily originate from the Southern Ocean and are useful chemical tracers of marine air (Davis et al., 1998 and references therein).

### 3.2.2. Source regions from outside of Antarctica

Fig. 6 shows the 500 hPa geopotential height distribution for December 2003. On a constant pressure surface, a high (low) geopotential height



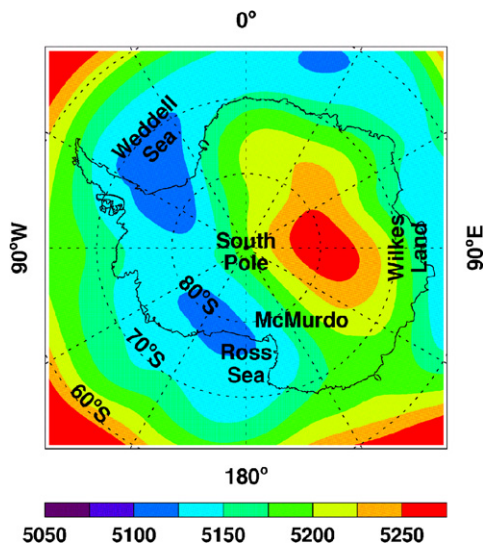


Fig. 6. Polar MM5 assimilated monthly mean geopotential heights at 500 hPa in December 2003.

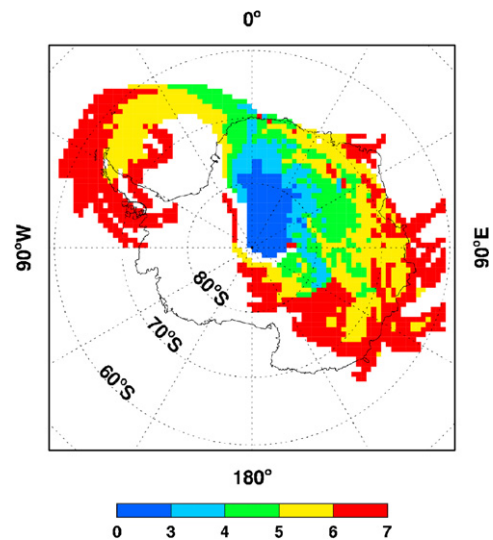


Fig. 7. The coverage of 7-day back-trajectories from the SP. Grids with color represent the mean time backward in days.

anomaly represents a high (low)-pressure system, and in the southern hemisphere, the circulation of high-pressure systems is cyclonic. The circulation during December of 2003 was characterized by low-pressure systems over the Weddell and Ross Seas, a broad circumpolar low-pressure band to the east and a high-pressure system over East Antarctica. Among these systems, the low-pressure system over Weddell Sea and the high-pressure system over East Antarctica had direct impacts on the transport of air parcels into SP. Prior studies have highlighted the importance of low-pressure systems over the Ross Sea and ice shelf in terms of marine air flow to SP (Harris, 1992; Hogan, 1997), but the trajectories calculated for the ANTCI mission in 2003 do not support strong transport from the Ross Sea.

The 7-day back-trajectories to SP are plotted in Fig. 7, and a major portion of air mass transport over East Antarctica can be seen as due to the strong high-pressure system. Transport from the Southern Ocean to SP mostly comes from 345° through 0° to 120°E from the Weddell Sea and the coast of Wilkes Land, respectively. The former transport is driven by the low-pressure system over the Weddell Sea that extends inland. The latter transport initially is driven by the circumpolar low-pressure system and then by the high-pressure system over East Antarctica. The average transport time from the Weddell Sea to the SP is typically 5 days; whereas 6 or more days are required for transport from the coast of Wilkes Land.

In part because of the elevation of SP, transport from the Southern Ocean generally starts at an altitude of 2–3 km, and the degree of marine influence on the plateau depends on the uplifting of surface marine air to this height. Fig. 6 shows that the low-pressure system was much stronger over the Weddell Sea than off the coast of Wilkes Land, resulting in stronger lifting of marine air. Furthermore, transport was faster from the Weddell Sea, reducing the effect of mixing with non-marine air. Thus, in general, one would expect to see stronger marine influence in air masses transported from the Weddell Sea, a trend actually supported by the measurements.

**3.2.2.1. Aerosol transport from the Weddell Sea.** We used trajectory analyses to investigate several specific aerosol events at the SP. One of these was from 9 to 11 December when the sulfate concentrations reached levels  $> 200 \text{ ng m}^{-3}$ , thus substantially exceeding the mean value for the entire intensive sampling period of  $145 \text{ ng m}^{-3}$ . By contrast, the measured  $\text{f-NO}_3^-$  concentration during this same period dropped below  $200 \text{ ng m}^{-3}$ , a value considerably less than the mean of  $280 \text{ ng m}^{-3}$ . A plot of the cumulative distribution functions for sulfate and nitrate (Fig. 8) shows that the sulfate values during the 9–11 December period ranked among highest of the study (upper 15% of the data) while the nitrate values were among the lowest (10–40%).

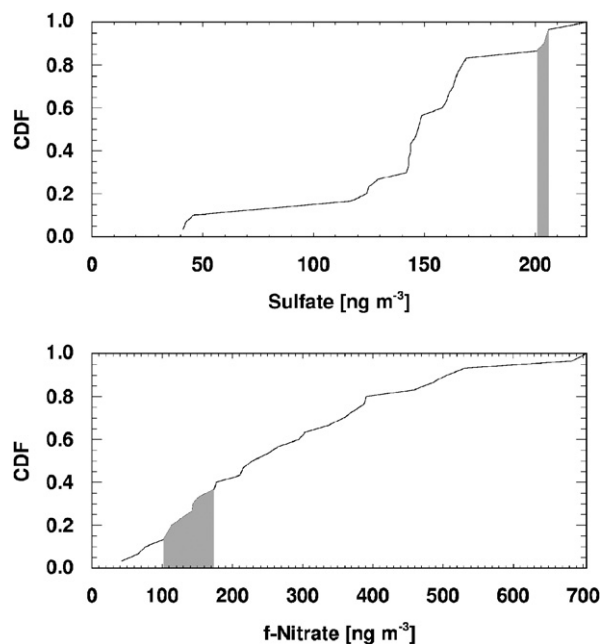


Fig. 8. Cumulative distribution functions (CDF) for sulfate and f-nitrate. The CDF shows the fraction of data points that are less than a given concentration. Shaded areas illustrate the ranges of sulfate and nitrate concentrations for 9–11 December 2003.

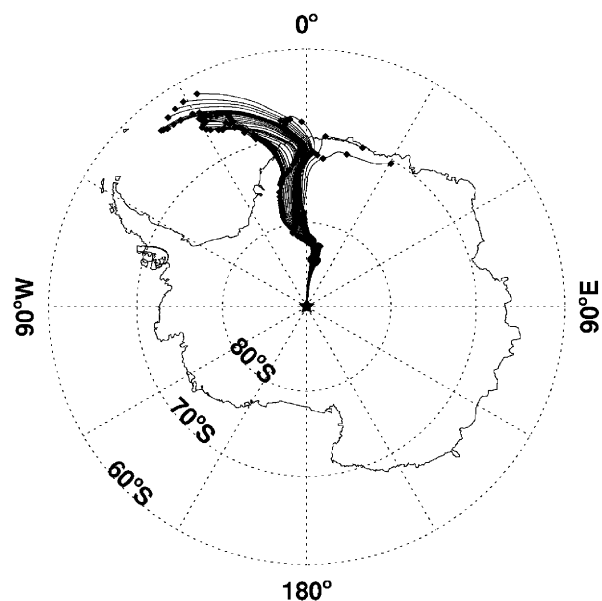


Fig. 9. All 5-day back-trajectories reaching the Southern Ocean. Trajectories are calculated every 1 h.

To better understand the sources and transport of aerosols, we focused on 5-day back-trajectories that originated over or near the Weddell Sea (Fig. 9). The contrasting trends in sulfate and nitrate clearly reflect the oceanic origin of the aerosol sulfate and

the low levels of nitrate emitted from the Weddell Sea; the results also imply that there was a relatively small influence of snow-derived  $\text{NO}_x$  on these samples. The trajectory model indicates that surface air was elevated to an altitude of 2–3 km by a low-pressure system before the air was transported to SP.

The results of the trajectory analyses are consistent with SeaWiFS satellite images, which reveal persistently high chlorophyll levels (implying high phytoplankton densities) in the Southern Ocean near Antarctica during the spring and summer,<sup>1</sup> particularly in the area of the Weddell Sea. Furthermore, the timing of the elevated  $\text{nss-SO}_4^{2-}$  at SP is synchronous with the arrival of marine air parcels from the Weddell Sea region. Although there is not necessarily a quantitative relationship between chlorophyll/phytoplankton levels and DMS concentrations in seawater, an overall general trend often does exist (Saltzman et al., 1983; DiTullio and Smith, 1995), and taken in combination with direct observations, one can reasonably conclude that the Weddell Sea is an important source for DMS. Due to the rapid oxidation of DMS released into the atmosphere, this marine region thus defines a probable source region for MSA and  $\text{nss-SO}_4^{2-}$  that reach SP and more generally the plateau.

The relatively low SP  $\text{f-NO}_3^-$  concentrations observed over these 3 days imply small contributions of nitrate from marine sources. As discussed later, more significant sources for reactive nitrogen exist on the plateau, and they are most likely responsible for the observations showing that nitrate concentrations increase as one moves from coastal sites (e.g., 25–30  $\text{ng m}^{-3}$ , Savoie et al., 1993; ~50  $\text{ng m}^{-3}$ , Wagenbach et al., 1998) to plateau sites such as SP (39–250  $\text{ng m}^{-3}$ ; this study and Arimoto et al., 2004a). Collectively, these results point to a small contribution of nitrogen from marine sources in the form of nitrate, but it does not rule out the possibility of a marine source of nitrogen that may be in a reduced oxidation state as suggested by Davis et al. (this issue) and Mopper and Zika (1987).

3.2.2.2. Transport from the Southern Ocean near Wilkes Land. With an extension of the transport timeframe to 6–7 days (Fig. 7), many of the

<sup>1</sup>Images are available online at <http://oceancolor.gsfc.nasa.gov/>.

air-trajectories that terminated at SP were found to have passed over the Southern Ocean near Wilkes Land (90–120°E). Aerosol concentrations at SP are found to be more variable for this group of trajectories compared with the case for the Weddell Sea, and the explanation for the observed patterns is not nearly so straightforward. There were some days when both  $f\text{-NO}_3^-$  and  $\text{nss-SO}_4^{2-}$  concentrations were high (4 of the 5 days with the highest  $f\text{-NO}_3^-$  concentrations are associated with air masses from this direction); indeed, one of the days in this trajectory group which had high  $f\text{-NO}_3^-$  also had one of the highest  $\text{nss-SO}_4^{2-}$  concentrations. Yet on other days with these trajectories both  $\text{nss-SO}_4^{2-}$  and  $f\text{-NO}_3^-$  were low.

Although complex at first glance, we suggest that these results can be partially, if not totally, understood in terms of the previously identified factors that have a critical influence on the local levels of  $\text{NO}_x$  and  $\text{NO}_y$ . The basis for this argument is that all evidence continues to point to near-field emissions of reactive nitrogen as the dominant source for  $f\text{-NO}_3^-$  (Davis et al., 2001, 2004, 2006; Neff et al., 2007; Helmig et al., 2007). One of the more interesting characteristics of air parcels that passed over Wilkes Land is that they have historically provided the highest levels of NO observed at SP (Davis et al., this issue). Those studies showed elevated  $\text{NO}_x$  mixing ratios in air from this part of the plateau, and the authors proposed that drainage flow from the area affects lower elevations, including SP. During the drainage process,  $\text{NO}_x$  can accumulate in the air through both physical and non-linear chemical processes. High NO rapidly leads to high levels of  $\text{HNO}_3$  and  $\text{HO}_2\text{NO}_2$ , and these in turn give rise to high  $f\text{-NO}_3^-$ .

The contrasting case, that is, low  $f\text{-NO}_3^-$  can be understood in terms of the major role played by the depth of the PBL. As the dominant source for  $\text{NO}_x$  on the plateau is the photodenitrification of the snow-pack, any substantial increase in PBL depth typically results in a major decrease in NO (Davis et al., 2004, this issue; Neff et al., 2007), and hence, by extension lower  $f\text{-NO}_3^-$ .

The low  $\text{nss-SO}_4^{2-}$  levels in the samples with these trajectories follow from the fact that the air masses that passed over Wilkes Land were profoundly affected by their interactions with the snow surface, including particle deposition, as they were transported over a distance of >1000 km. On the other hand, if the air initially had significant contact with the Southern Ocean beyond Wilkes Land, there

would be good reason to believe that significant amounts of DMS would have been incorporated into the air parcels. If so, as discussed above, the DMS would be rapidly oxidized to  $\text{SO}_2$  (due to highly elevated levels of OH, see Davis et al., this issue; Wang et al., 2007; Mauldin et al., 2001, 2004, 2007) and finally to  $\text{nss-SO}_4^{2-}$  well before arriving at SP.

It is also possible that the Southern Ocean near Wilkes Land is influenced by continental sources of nitrate. In this case, an examination of the mean activity of  $^{210}\text{Pb}$ , an indicator of air from distant continental sources, reveals relatively high levels of this radionuclide ( $0.18 \text{ mBq m}^{-3}$ ) during the ANTCI intensive period. However, there was no clear correlation between  $f\text{-NO}_3^-$  and  $^{210}\text{Pb}$  ( $r = 0.25$ ), which suggests variability in the strengths of the continental sources. Nevertheless, one cannot totally rule out some degree of impact from one or more continental source(s) since high concentrations of anthropogenic trace elements were found in some samples having high  $f\text{-NO}_3^-$ .

#### 4. Conclusions

The concentrations of  $\text{nss-sulfate}$  and MSA and the  $\text{MSA/nss-SO}_4^{2-}$  ratios during ANTCI were comparable to those during the two ISCAT campaigns, but the average  $f\text{-NO}_3^-$  concentration during ANTCI was considerably higher than for either of the earlier ISCAT missions. Trace-element data and trajectory analyses suggest that there were stronger marine influences and more long-range transport of continental aerosols to SP in 2003 compared with 2000.

The long-range transport of marine air is affected both by low-pressure systems over the ocean and by the high-pressure system over the polar plateau. Low-pressure systems have the potential for injecting air masses rich in  $\text{nss-sulfate}$ , sea salt, DMS, MSA and other substances of biogenic origin into the free troposphere (>2 km), and under these circumstances, transport to SP can occur. Even though we cannot exclude the possibility that transport also occurs at lower altitudes, aerosol deposition would reduce its efficiency for transporting particles, and strong katabatic winds would make low-altitude transport to the high plateau difficult. In addition, we found that the back-trajectories often followed the edge of a persistent high-pressure system over the Antarctic Plateau.

Two potential source areas for nss-SO<sub>4</sub><sup>2-</sup> were identified through trajectory analyses. The first was the Weddell Sea and the second the Southern Ocean near Wilkes Land (90–120°E). In the case of the former the transport time is <5 days, whereas it can be >6 days from the Southern Ocean near Wilkes Land. Modeling studies by Davis et al. (1998) indicate that if, as we have concluded, the transport of biogenic sulfur occurs primarily in the free troposphere/buffer layer, the resulting MSA/nss-SO<sub>4</sub><sup>2-</sup> ratio would likely be low due to the absence of heterogeneous DMS oxidation processes; this is consistent with both ISCAT and ANTCI results.

Filterable nitrate was found to be mainly composed of nitric acid, and while there is evidence that some nitrate might have been transported to SP from distant sources and that up to 35% of the f-NO<sub>3</sub><sup>-</sup> is associated with sea salt, the preponderance of the data shows that local emissions of NO<sub>x</sub> from the snow are a far more important source of f-NO<sub>3</sub><sup>-</sup> overall. The fact that high nitrate events at SP were linked to air masses arriving from the east is consistent with the idea that the drainage of NO-rich air from the higher elevations of Wilkes Land provides a major source of nitrogen species to SP. Occasional concurrent high nss-SO<sub>4</sub><sup>2-</sup> with high f-NO<sub>3</sub><sup>-</sup> events indicate that some air parcels moving onto the plateau from the Southern Ocean can contain elevated levels of DMS. In the latter case, the DMS can be rapidly oxidized by plateau OH as the parcel moves toward the SP. When air masses move into the plateau from the Weddell Sea, they are typically rich in nss-SO<sub>4</sub><sup>2-</sup> due to recently injected DMS, but when sampled at SP, they are typically low in nitrate because the air parcel has had limited contact with the nitrogen-rich plateau region.

### Acknowledgments

We thank the NOAA staff at the South Pole Station, especially Stephanie Koes and Glen Kinoshita, for their cooperation, support and dedication during the ANTCI field operations, and we appreciate the help of Thomas Mefford who provided meteorological data. We also thank Joe Fraire for preparing the samples for <sup>210</sup>Po analyses and Jon Seelig for his help preparing several of the figures. This material is based on work supported by the National Science Foundation under Grant Nos. NSF OPP 0229605 (NMSU) and 0230246 (GIT).

Any opinions, findings and conclusions or recommendations expressed in this material are those of the authors and do not necessarily reflect the views of the National Science Foundation.

### References

- Arimoto, R., Nottingham, A.S., Webb, J., Schloesslin, C.A., Davis, D., 2001. Non-sea salt sulfate and other aerosol constituents at the South Pole during ISCAT. *Geophysical Research Letters* 28, 3645–3648.
- Arimoto, R., Hogan, A., Grube, P., Davis, D., Webb, J., Schloesslin, C., Sage, S., 2004a. Major ions and radionuclides in aerosol particles from the South Pole during ISCAT-2000. *Atmospheric Environment* 38, 5473–5484.
- Arimoto, R., Schloesslin, C., Davis, D., Hogan, A., Grube, P., Fitzgerald, W., Lamborg, C., 2004b. Lead and mercury in aerosol particles from the South Pole collected during ISCAT-2000. *Atmospheric Environment* 38, 5485–5491.
- Balkanski, Y.J., Jacob, D.J., Gardner, G.M., Graustein, W.C., Turekian, K.K., 1993. The transport and residence times of tropospheric aerosols inferred from a global three-dimensional simulation of <sup>210</sup>Pb. *Journal of Geophysical Research* 98, 20,573–20,586.
- Berresheim, H., Eisele, F.L., 1998. Sulfur chemistry in the Antarctic troposphere experiment—an overview of project SCATE. *Journal of Geophysical Research* 103, 1619–1627.
- Brimblecombe, P., Clegg, S.L., 1988. The solubility and behaviour of acid gases in the marine aerosol. *Journal of Atmospheric Chemistry* 7, 1–18.
- Bromwich, D.H., Cassano, J.J., Klein, T., Heinemann, G., Hines, K.M., Steffen, K., Box, J.E., 2001. Mesoscale modeling of katabatic wind over Greenland with the polar MM5. *Monthly Weather Review* 129, 2090–2309.
- Brooks, S., Arimoto, R., Lindberg, S., Southworth, G., this issue. Antarctic polar plateau snow surface conversion of deposited oxidized mercury to gaseous elemental mercury with fractional long-term burial. *Atmospheric Environment*, doi:10.1016/j.atmosenv.2007.05.029.
- Courant, R., Friedrichs, K., Lewy, H., 1928. Über die partiellen differenzgleichungen der mathematischen physik. *Mathematische Annalen* 100, 32–74.
- Davis, D., Chen, G., Kasibhatla, P., Jefferson, A., Tanner, D., Eisele, F., Lenschow, D., Neff, W., Berresheim, H., 1998. DMS oxidation in the Antarctic marine boundary layer: comparison of model simulations and field observations of DMS, DMSO, DMSO<sub>2</sub>, H<sub>2</sub>SO<sub>4</sub>(g) MSG(g) and MSA(p). *Journal of Geophysical Research* 103, 1657–1678.
- Davis, D., Buhr, M., Nowak, J., Chen, G., Arimoto, R., Hogan, A., Eisele, F., Mauldin, L., Tanner, D., Shetter, R., Lefer, B., McMurry, P., 2001. Unexpected high levels of NO observed at the South Pole. *Geophysical Research Letters* 28, 3625–3628.
- Davis, D., Chen, G., Buhr, M., Crawford, J., Lenschow, D., Lefer, B., Shetter, R., Eisele, F., Mauldin, L., Hogan, A., 2004. South Pole NO chemistry: an assessment of factors controlling variability and absolute levels. *Atmospheric Environment* 38, 5375–5388.
- Davis, D.D., Seelig, J., Huey, G., Crawford, J., Chen, G., Wang, Y., Buhr, M., Helmig, D., Neff, W., Blake, D., Arimoto, R.,

- Eisele, F., this issue. A reassessment of Antarctic plateau reactive nitrogen based on ANTCI 2003 airborne and ground base measurements, submitted for publication.
- DiTullio, G.R., Smith Jr., W.O., 1995. Relationship between dimethylsulfide and phytoplankton pigment concentrations in the Ross Sea, Antarctica. *Deep-Sea Research I* 42, 873–892.
- Eisele, F., Davis, D.D., Helmig, D., Oltmans, S.J., Neff, W., Huey, G., Chen, G., Crawford, J., Arimoto, R., Buhr, M., Mauldin, L., Hutterli, M., Dibb, J., Blake, D., Roberts, J., Wang, Y., Tan, D., Flocke, F., this issue. Antarctic tropospheric chemistry investigation (ANTCI) 2003 overview. *Atmospheric Environment*, in press, doi:10.1016/j.atmosenv.2007.04.013.
- Gerasopoulous, E., Zerefos, C.S., Papastefanou, C., Zanis, P., O'Brien, K., 2003. Low-frequency variability of beryllium-7 surface concentrations over the Eastern Mediterranean. *Atmospheric Environment* 37, 1745–1756.
- Gragnani, R., Smiraglia, C., Stenni, B., Torcini, S., 1998. Chemical and isotopic profiles from snow pits and shallow firn cores on Campbell Glacier, northern Victoria Land, Antarctica. *Annals of Glaciology* 27, 679–684.
- Harris, J.M., 1992. An analysis of 5 day midtropospheric flow patterns for the South Pole, 1985–1989. *Tellus Series B* 44, 409–421.
- Helmig, D., Johnson, B., Oltmans, S.J., Neff, W., Eisele, F., Davis, D.D., 2007. Elevated ozone in the boundary-layer at South Pole. *Atmospheric Environment*, in press, doi:10.1016/j.atmosenv.2006.12.032.
- Hogan, A.Q., 1997. A synthesis of warm air advection to the South Polar Plateau. *Journal of Geophysical Research* 102, 14,009–14,020.
- Kärkäs, E., Teinilä, K., Virkkula, A., Aurela, M., 2005. Spatial variations of surface snow chemistry during two austral summers in western Dronning Maud Land Antarctica. *Atmospheric Environment* 39, 1405–1416.
- Maenhaut, W., Zoller, W.H., Duce, R.A., Hoffman, G.L., 1979. Concentration and size distribution of particulate trace elements in the South Polar atmosphere. *Journal of Geophysical Research* 84, 2421–2431.
- Mauldin, R.L., Eisele, F.L., Tanner, D.J., Kosciuch, E., Shetter, R., Lefer, B., Hall, S.R., Nowak, J.B., Buhr, M., Chen, G., Wang, P., Davis, D., 2001. Measurements of OH, H<sub>2</sub>SO<sub>4</sub>, and MSA at the South Pole during ISCAT. *Geophysical Research Letters* 28, 3629–3632.
- Mauldin III, R.L., Kosciuch, E., Henry, B., Eisele, F.L., Shetter, R., Lefer, B., Chen, G., Davis, D., Huey, G., Tanner, D., 2004. Measurements of OH, HO<sub>2</sub> + RO<sub>2</sub>, H<sub>2</sub>SO<sub>4</sub>, and MSA at the South Pole during ISCAT-2000. *Atmospheric Environment* 38, 5423.
- Mauldin III, R.L., Kosciuch, E., Eisele, F., Crawford, J., Huey, G., Tanner, D., Sojstead, S., Blake, D., Davis, D., 2007. OH, H<sub>2</sub>SO<sub>4</sub>, and MSA measurements and correlations during ANTCI-2003. *Atmospheric Environment*, submitted for publication.
- Mopper, K., Zika, R.G., 1987. Free amino acids in marine rains: evidence for oxidation and potential role in nitrogen cycling. *Nature* 325, 246–249.
- Neff, W.D., Helmig, D., Grachev, A., Davis, D., 2007. A study of boundary layer behavior associated with high NO concentrations at the South Pole using a minisodar, tethered balloon, and sonic anemometer. *Atmospheric Environment*, in press, doi:10.1016/j.atmosenv.2007.01.033.
- Piel, C., Weller, R., Huke, M., Wagenbach, D., 2006. Atmospheric methane sulfonate and non-sea-salt sulfate records at the European Project for Ice Coring in Antarctica (EPICA) deep-drilling site in Dronning Maud Land, Antarctica. *Journal of Geophysical Research* 111, D03304.
- Press, H.W., Fannery, B.P., Teukolsky, S.A., Vetterling, W.T., 1992. *Numerical Recipes in Fortran 77: The Art of Scientific Computing*, second ed. Cambridge University Press, Cambridge, UK.
- Saltzman, E.S., Savoie, D.L., Zika, R.G., Prospero, J.M., 1983. Methane sulfonic acid in the marine atmosphere. *Journal of Geophysical Research* 88, 10,897–10,902.
- Savoie, D.L., Prospero, J.M., Saltzman, E.S., 1989. Nitrate, non-sea-salt sulfate and methanesulfonate over the Pacific Ocean. In: Riley, J.P., Chester, R., Duce, R.A. (Eds.), *Chemical Oceanography*, vol. 10. Academic Press, London, pp. 219–250.
- Savoie, D.L., Prospero, J.M., Larsen, R.J., Huang, F., Izaguirre, M.A., Huang, T., Snowdon, T.H., Custals, L., Sanderson, C.G., 1993. Nitrogen and sulfur species in Antarctic aerosols at Mawson, Palmer Station and Marsh (King George Island). *Journal of Atmospheric Chemistry* 17, 95–122.
- Schaap, M., Spindler, G., Schulz, M., Acker, K., Maenhaut, W., Berner, A., Wieprecht, W., Streit, N., Müller, K., Brüggemann, E., Chi, X., Putaud, J.-P., Hitzemberger, R., Puxbaum, H., Baltensperger, U., Ten Brink, H.M., 2004. Artifacts in the sampling of nitrate studied in the “INTERCOMP” campaigns of EUROTRAC-AEROSOL. *Atmospheric Environment* 38, 6487–6496.
- Sjostedt, et al., this issue. Measurement of HNO<sub>3</sub> and HNO<sub>4</sub> at the South Pole during the ANTCI-2003 summer field campaign: implications for reactive nitrogen speciation in polar regions. *Atmospheric Environment*, submitted for publication.
- Su, C., Huh, C., 2002. Atmospheric <sup>210</sup>Po anomaly as a precursor of volcano eruptions. *Geophysical Research Letters* 29, 1070.
- Udisti, R., Becagli, S., Benassai, S., Castellano, E., Fattori, I., Innocenti, M., Migliori, A., Traversi, R., 2004. Atmosphere-snow interaction by a comparison between aerosol and uppermost snow-layers composition at Dome C, East Antarctica. *Annals of Glaciology* 29, 53–61.
- Wagenbach, D., Curroz, F., Mulvaney, R., Keck, L., Minikin, A., Legrand, M., Hall, J.S., Wolff, E.W., 1998. Sea-salt aerosol in coastal Antarctic regions. *Journal of Geophysical Research* 103, 10,961–10,974.
- Wang, Y., Choi, Y., Zeng, T., Davis, D., Buhr, M., Huey, L.G., Neff, W., 2007. Assessing the photochemical impact of snow NO<sub>x</sub> emissions over Antarctica during ANTCI-2003. *Atmospheric Environment* 41, 3944–3958.
- Zeng, T., 2005. Three-dimensional modeling analysis of photochemistry in the Arctic and at northern mid-latitudes. Ph.D. Thesis. Georgia Institute of Technology, Atlanta, 203pp.